JCS ePress online publication date 2 February 2010

An RbAp48-like gene regulates adult stem cells in planarians

Lucia Bonuccelli[1], Leonardo Rossi[1], Annalisa Lena[1], Vittoria Scarcelli[1], Giuseppe Rainaldi[2], Monica Evangelista[2], Paola Iacopetti[1], Vittorio Gremigni[1] and Alessandra Salvetti[1,*]

[1]Dipartimento di Morfologia Umana e Biologia Applicata, Università di Pisa, Pisa, Italy
[2]Istituto di Fisiologia Clinica, Laboratorio di Terapia Genica e Molecolare, CNR, Pisa, Italy
*Author for correspondence (a.salvetti@biomed.unipi.it)

Accepted 21 November 2009
Journal of Cell Science 123, 690-698

doi:10.1242/jcs.053900

Summary

Retinoblastoma-associated proteins 46 and 48 (RbAp46 and RbAp48) are factors that are components of different chromatin-modelling complexes, such as polycomb repressive complex 2, the activity of which is related to epigenetic gene regulation in stem cells. To date, no direct findings are available on the in vivo role of RbAp48 in stem-cell biology. We recently identified *DjRbAp48* – a planarian (*Dugesia japonica*) homologue of human *RBAP48* – expression of which is restricted to the neoblasts, the adult stem cells of planarians. In vivo silencing of *DjRbAp48* induces lethality and inability to regenerate, even though neoblasts proliferate and accumulate after wounding. Despite a partial reduction in neoblast number, we were always able to detect a significant number of these cells in *DjRbAp48* RNAi animals. Parallel to the decrease in neoblasts, a reduction in the number of differentiated cells and the presence of apoptotic-like neoblasts were detectable in RNAi animals. These findings suggest that *DjRbAp48* is not involved in neoblast maintenance, but rather in the regulation of differentiation of stem-cell progeny. We discuss our data, taking into account the possibility that DjRbAp48 might control the expression of genes necessary for cell differentiation by influencing chromatin architecture.

Key words: Retinoblastoma-associated protein 48, Neoblast, RNAi, Differentiation, Invertebrate

Introduction

Freshwater planarians (Platyhelminthes) are able to regenerate complete organisms in only two weeks independently from the amputation site and also from a very tiny fragment of their body (Morgan, 1898). This extraordinary regeneration capability derives from the presence of a heterogeneous population of pluripotent adult stem cells, called neoblasts, which are maintained throughout the animal life (Baguñà et al., 1989; Rossi et al., 2008). The presence of neoblasts, coupled with the successful application of molecular, cellular and genomic approaches, including the possibility of applying RNA interference (RNAi) to in vivo functional studies, makes planarians a sound model system for in vivo studies of pluripotent adult stem cells and regeneration.

Neoblasts are small cells (5-10 μm diameter), with a large nucleus surrounded by a scanty rim of undifferentiated cytoplasm. They are spread throughout the parenchyma (a mesenchymal tissue) and also accumulate in clusters along the midline and the dorso-lateral parenchyma. These stem cells are absent only in the proximal part of the head and in the pharynx (Orii et al., 2005; Salvetti et al., 2000). Neoblasts give rise to the regenerative blastema and, in intact animals, are involved in tissue homeostasis, continuously replacing specialized cells lost during physiological cell turnover (Rossi et al., 2008). Neoblasts are the only proliferating cells in asexual planarians and are destroyed a few days after treatment with lethal doses of X-rays, whereas differentiated cells are unaffected at the same time after treatment with such X-ray doses (Wolff and Dubois, 1948).

Taking advantage of this possibility, we previously compared the transcriptional profile of planarians deprived of stem cells with that of 'wild-type' animals by microarray analysis. We identified a neoblast signature composed of 44 neoblast-specific genes that principally belong to chromatin-modelling and post-transcriptional regulation functional categories (Rossi et al., 2007). Among the chromatin-modelling factors, we found a planarian homologue of mammalian RbAp48, initially identified as a retinoblastoma (Rb)-binding protein (Qian et al., 1993), which is a WD40 repeat protein that is conserved in animals and plants. RbAp48 and its homologue RbAp46 are components of several complexes involved in chromatin metabolism, including NURD (nucleosome remodelling histone deacetylase complex), CAF-1, histone acetyltransferases and histone-deacetylase (HDAC)-containing complexes (Parthun et al., 1996; Philpott et al., 2000; Qian et al., 1993; Taunton et al., 1996; Verreault et al., 1996). Because all these complexes have histones as their substrates, the general hypothesis is that RbAp46 and RbAp48 connect histones with these complexes (Loyola and Almouzni, 2004). Depending on subunit composition, these protein complexes are capable of affecting all stages of chromatin metabolism. Consistent with this role, developmental studies in plants have suggested that RbAp48 proteins might play a role in maintaining epigenetic changes throughout cell division (Hennig et al., 2003). Moreover, these factors also play a role in the regulation of Ras-regulated pathways in *Caenorhabditis elegans*, *Saccharomyces cerevisiae* and mammalians (Lu and Horvitz, 1998; Qian et al., 1993; Qian et al., 1995; Ruggieri et al., 1989; Scuto et al., 2007). The Ras pathway is involved in several important cellular processes, including proliferation, apoptosis, cytoskeletal organization and differentiation (Bar-Sagi and Hall, 2000; Cox and Der, 2003; Downward, 2003; Hancock, 2003; Shields et al., 2000). Another complex containing RbAp46 and RbAp48 factors is polycomb repressive complex 2 (PRC2), a histone-methyltransferase-containing complex whose activity is related to epigenetic gene regulation in stem cells. Although several reports

implicate PRC2 in the maintenance of stem cells (Azuara et al., 2006; Boyer et al., 2006a; Boyer et al., 2006b; Kamminga et al., 2006; Lee et al., 2006), recent findings indicate that PRC2 is dispensable for embryonic stem-cell pluripotency and that it might be important for differentiation and maintenance of multipotency in later progenitor cells (Chamberlain et al., 2008). Despite these data concerning the role of PRC2 in stem cells, no direct findings are available to date on the in vivo role of RbAp48 factors in stem-cell biology.

In this paper, we investigate the functional role of planarian (*Dugesia japonica*) *DjRbAp48* by RNAi analysis. We found that *DjRbAp48* RNAi is lethal in both regenerating and intact planarians. Although neoblasts are activated and accumulate below the epithelium after wounding, the regeneration capability is affected by *DjRbAp48* silencing. Interestingly, we observed the presence of apoptotic-like neoblasts below the wound of RNAi animals. Intact *DjRbAp48*-silenced animals also show the presence of apoptosis, together with a progressive reduction in the number of neoblasts and differentiated cells. We propose that *DjRbAp48* is involved in neoblast differentiation and discuss this hypothesis on the basis of our findings.

Results

DjRbAp48 is a WD40-like gene expressed in neoblasts

We investigated the function of the gene corresponding to the EST clone Gi32900731, which is similar to the retinoblastoma-binding protein Rbp4, previously identified in a neoblast signature (Rossi et al., 2007). First, we completed the sequence of this clone and named the full-length gene *DjRbAp48*. *DjRbAp48* encodes a putative protein that contains typical multiple WD40 repeats in its C-terminal region (residues 210 to 249; 260 to 299; 306 to 345; 350 to 389; 407 to 446); this allows us to consider it a new member of the WD40 protein family (Neer et al., 1994). The WD40 protein most closely related (BLASTX E-value: 0.0) to DjRbAp48 is *Danio rerio* retinoblastoma-binding protein 4 (Rbbp-4).

DjRbAp48 is expressed in neoblasts and its expression pattern is very similar to that of the neoblast molecular marker *DjMCM2* in intact planarians (Rossi et al., 2007). During regeneration, *DjRbAp48* transcripts are located close to the wound epithelium 1 day after transection and are detected in the blastema region after 2-3 days (supplementary material Fig. S1).

DjRbAp48 role during regeneration

To investigate the function of *DjRbAp48* in neoblast biology, we analyzed the effect of *DjRbAp48* RNAi during regeneration. Planarians amputated 7 days after the first dsRNA injection were able to form a blastema on the second day of regeneration but, starting 15 days after transection, they began to show reduced motility and several defects, such as curling and tissue regression (30/30); 40 days after transection, all RNAi animals were dead (data not shown). Interestingly, planarians amputated 20 days after the first dsRNA injection never formed a blastema (data not shown).

When the blastema was removed from 3-day-old regenerating animals (second transection), head fragments (n=50) injected with *DjRbAp48* dsRNA did not initiate the second regeneration process (Fig. 1A,B). These RNAi animals did not give rise to a blastema even 14 days after transection (Fig. 1D), whereas control animals had completely regenerated the missing body parts (Fig. 1C). Tail fragments injected with *DjRbAp48* dsRNA showed a delay in blastema production with respect to controls, and regenerated an abnormal, small head, usually with a single eye (supplementary material Fig. S2). These tail fragments were not able to produce a blastema 3 days after the fourth amputation (data not shown). RNAi fragments lysed 30 days after the second amputation (50/50). On the basis of these findings, planarians at the second regeneration were used in the following experiments.

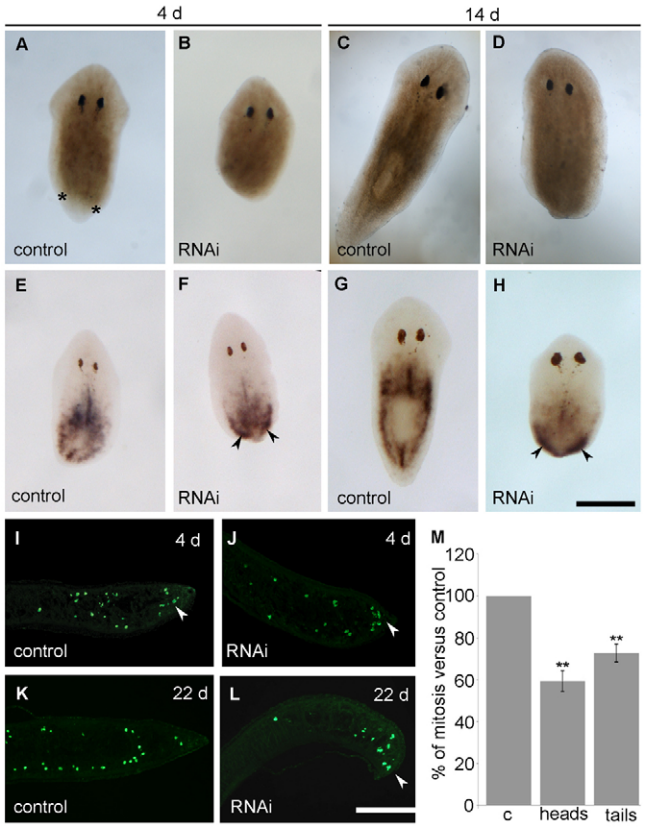

Fig. 1. Effect of *DjRbAp48* RNAi during tissue regeneration. (**A-D**) Brightfield images of injected organisms at different days (d) after the second transection. In *DjRbAp48*-silenced planarians (RNAi), no blastema is produced. The blastema is indicated by two asterisks in a control animal. (**E-H**) *DjMCM2* expression visualized by whole-mount in situ hybridization in regenerating RNAi and control planarians. Arrowheads indicate *DjMCM2*-positive cells accumulated below the wound epithelium. (**I-L**) Immunostaining performed using the anti-H3P antibody on longitudinal sections obtained from RNAi head fragments and control planarians. Arrowheads indicate mitotic cells accumulated below the wound epithelium. (**M**) Analysis of mitotic cells in control (c) and RNAi head (heads) and tail (tails) fragments. The number of cells able to enter the M-phase of the cell cycle in a temporal window of six hours was analyzed. Values are expressed as percentages with respect to the control planarians, to which the arbitrary value of 100% has been assigned. Each value represents the mean ± standard deviation of three independent samples counted in duplicate. **Significant at P<0.01. Statistical significance was assessed by Student's t-test. Scale bars: 1 mm (A-H); 150 μm (I-L).

To understand whether the inability of *DjRbAp48* RNAi planarians to form a blastema was due to a loss of neoblasts, we analyzed the expression pattern of the neoblast molecular marker *DjMCM2* (Salvetti et al., 2000) in regenerating animals (Fig. 1E-H). Interestingly, a significant number of *DjMCM2*-expressing cells were present in *DjRbAp48* RNAi planarians 4 days after transection and also accumulated below the wound epithelium (Fig. 1F). This pattern is reminiscent of that normally observed in wild-type animals 2 days after transection (data not shown). Two weeks later, a

reduction in the number of *DjMCM2*-positive cells was observed in the parenchyma, but significant accumulation of positive cells was still detected below the wound epithelium (Fig. 1G,H).

Because a significant number of neoblasts were present in *DjRbAp48* RNAi planarians that are unable to produce a regenerative blastema, we wondered whether such neoblasts were able to proliferate. To this aim, we used the mitotic cell marker anti-phosphohistone H3 antibody (anti-H3P) (Newmark and Sánchez Alvarado, 2000; Wei et al., 1998) to count the number of cells able to enter the M-phase of the cell cycle. Although mitotic cells were detected both in the parenchyma and below the wound epithelium of amputated *DjRbAp48*-silenced planarians 4 days after cutting (Fig. 1I,J), the number of mitotic cells was reduced with respect to controls (Fig. 1M). At 22 days after transection, the mitotic neoblasts spread all over the parenchyma were strongly reduced in number in RNAi animals in comparison to controls, but several proliferating neoblasts still accumulated below the wound epithelium (Fig. 1K,L). We also investigated whether *DjRbAp48* RNAi might affect tissue differentiation during the regeneration of the head in tail-injected fragments able to produce a small blastema. To this aim, we analyzed the expression of *DjSyt* (Tazaki et al., 1999), *DjAHNAK* (Rossi et al., 2007) and *Djinx1* (Nogi and Levin, 2005), molecular markers of the nervous system, epidermis and gut, respectively, by whole-mount *in situ* hybridization. Although the RNAi tail fragments showed a significant number of neoblasts, RNAi animals regenerated a smaller nervous system in comparison to controls (supplementary material Fig. S2). In addition, we detected defects in gut regeneration (i.e. failure in regenerating the anterior gut branch), as well as reduced epithelial cell density, after *DjRbAp48* silencing (supplementary material Fig. S2).

Transmission electron microscopy (TEM) analysis of fragments injected with *DjRbAp48* dsRNA and unable to regenerate (n=5) showed the absence of neoblasts close to the wound epithelium (Fig. 2). In particular, RNAi-induced phenotypes devoid of a visible blastema had rare neoblasts, intermingled with some differentiated cells, and apoptotic-like cells showing chromatin condensation and margination below the wound epithelium (Fig. 2B). By contrast, numerous unspecialized cells (neoblasts) were observed in a corresponding region of control animals (Fig. 2A). Moreover, *DjRbAp48* RNAi animals showed large groups of polarized neoblasts that were accumulated further from the wound epithelium with respect to the clusters of apoptotic-like cells (Fig. 2D). These oriented neoblasts were located in a body region that probably corresponds to where clustered *DjMCM2*-positive cells were detected by in situ hybridization. The presence of apoptotic cells in RNAi animals was confirmed by the DNA diffusion assay, which was designed to enable quantification of cell death by apoptosis (Singh, 2005) (Fig. 2E). Using this method, apoptotic nuclei show

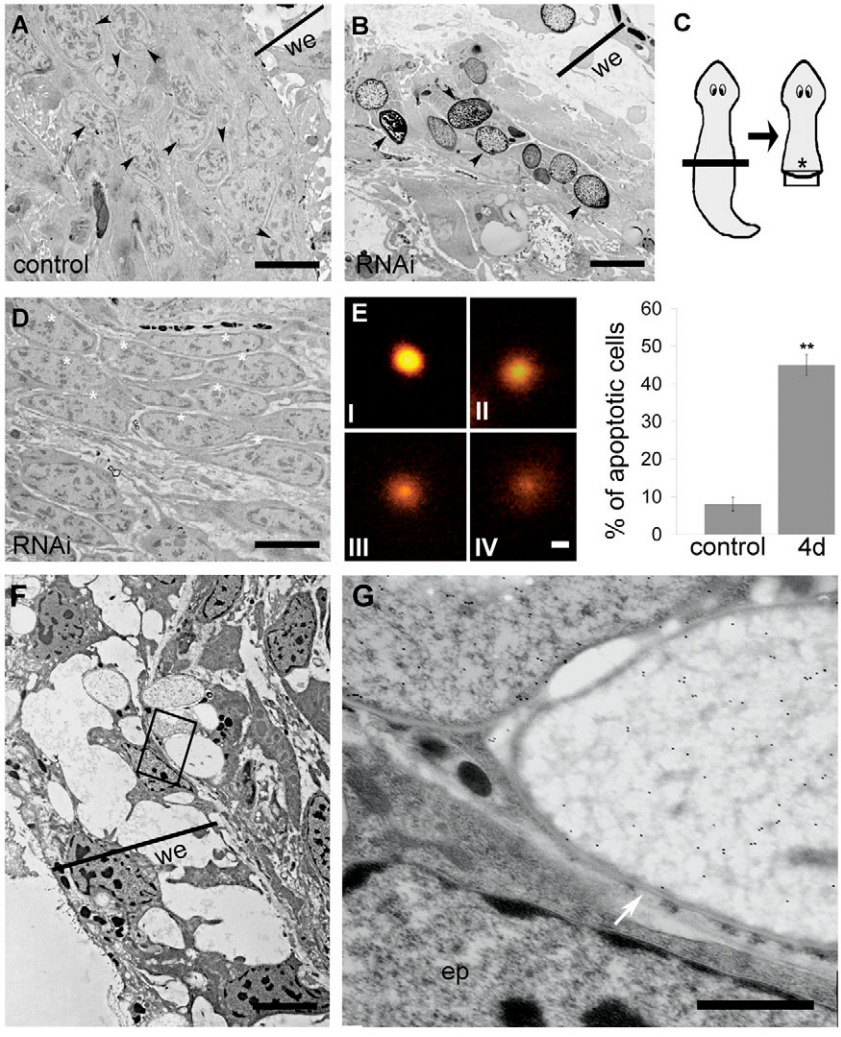

Fig. 2. Analysis of regenerating *DjRbAp48* RNAi planarians by TEM and DNA diffusion assay. (**A**,**B**) Micrographs of 3-day-old regenerating controls and *DjRbAp48*-silenced planarians (RNAi) showing no blastema. (A) Neoblasts accumulate below the wound epithelium of a control (arrowheads). (B) Apoptotic-like cells accumulate below the wound epithelium of RNAi animals (arrowheads). (**C**) Schematic drawing of a regenerating planarian. The black box indicates the body region corresponding to micrographs A and B. The asterisk indicates the body region corresponding to the image depicted in D. (**D**) Micrograph of a 3-day-old regenerating *DjRbAp48*-RNAi planarian showing oriented and accumulated neoblasts (asterisks). (**E**) DNA diffusion assay of nuclei obtained from control and *DjRbAp48* RNAi (4d) animals 4 days after the first injection. Dissociated cells were prepared from a pool of three planarians per sample. Nuclei classified as type IV were considered apoptotic. Values are expressed as the percentage of apoptotic nuclei with respect to the total counted nuclei. Each value is the average ± standard deviation of at least three independent samples counted in duplicate. For each sample, we counted 50 nuclei. **Significant at P<0.01. (**F**,**G**) Analysis of BrdU-positive cells by TEM. (F) Low-magnification image of the wound region of a 3-day-old regenerating *DjRbAp48*-silenced planarian injected with BrdU. The boxed area is enlarged in G. (G) Two apoptotic-like cells with clusters of gold particles in their nuclei and an epidermal cell (ep) with no gold particles in its nucleus. The white arrow indicates the nuclear envelope. we, wound epithelium. Statistical significance was assessed by Student's t-test. Scale bars: 5 μm (A,B); 6 μm (D); 10 μm (E); 4 μm (F); 1 μm (G).

a halo of granular DNA with hazy outer boundaries. Apoptotic cells can be distinguished from necrotic ones, as the latter exhibit unusually large, homogeneous nuclei with clearly defined boundaries (Singh, 2000).

To understand whether the clusters of apoptotic-like cells that accumulated below the wound region of regenerating RNAi animals were dying neoblasts, we injected BrdU into RNAi animals and then analyzed BrdU incorporation by TEM analysis. As neoblasts are the only proliferating cells in asexual planarians, we expected to find BrdU in neoblasts, in neoblast differentiating progeny and in some differentiated cells. We detected gold particles in the nuclei of clustered apoptotic-like cells located below the wound epithelium, but not in the nuclei of epithelial cells 3 and 6 days after RNAi (Fig. 2F), a time sufficient for epithelial cell differentiation (Newmark and Sánchez Alvarado, 2000). Fig. 2G shows the nuclear envelope and the chromatin structures of a BrdU-positive cell.

Role of *DjRbAp48* in intact animals

Intact planarians injected with *DjRbAp48* dsRNA began to die 42 days after the first injection and all animals were dead from the fiftieth day (n=50). Injected animals began to show reduced motility 30 days after the first microinjection, followed by curling and progressive head regression (Fig. 3A). No defects were observed in control animals and they survived for well over 9 weeks (n=25). As the RNAi phenotype is indicative of stem-cell loss, we analyzed the expression of some neoblast molecular markers, such as *DjMCM2* (Salvetti et al., 2000), *DjPiwi-1* (Rossi et al., 2006) and *Djnos* (Sato et al., 2006), in injected animals 20, 30 and 40 days after RNAi by whole-mount in situ hybridization (Fig. 3B). A progressive reduction in the number of *DjMCM2*-positive cells scattered throughout the parenchyma, as well as clustered in front of the pharynx and along the dorsal lateral lines, occurred in RNAi animals. Generally, we observed that neoblasts decreased in number more rapidly in the anterior body region than in the posterior body region of RNAi animals. *DjMCM2*-positive cells were always detected along the midline of the body posterior to the pharynx, as well as in animals showing head regression (Fig. 3B). Then, we counted the number of *DjMCM2*-positive cells in a population of dissociated cells obtained from both control and RNAi animals; the findings obtained confirmed the reduction in the number of neoblasts 20 days after RNAi treatment with respect to the controls (Fig. 4A). Similar results were obtained by analyzing the expression of *DjMCM2* by real-time reverse transcriptase (RT)-PCR in *DjRbAp48* RNAi planarians both 20 and 30 days after the first injection, confirming the presence of a significant, although reduced, number of neoblasts in RNAi animals in comparison to controls (Fig. 5A). *DjPiwi-1*-positive cells were detected along the dorsal body midline anterior to the pharynx at all times during analysis, as well as in phenotypes showing head regression (Fig. 3B). However, we failed to detect *DjPiwi-1*-expressing cells in RNAi animals with strong head regression (no eyes) (data not shown). Furthermore, we analyzed the distribution of the *nanos*-related gene *Djnos*, which is expressed in a subpopulation of neoblasts that are considered to be germline stem cells (Sato et al., 2006). At 20 days after RNAi, we observed a reduction in the number of *Djnos*-positive cells with respect to the controls, although clusters of *Djnos*-expressing cells were still detected posterior to the pharynx. At 40 days after injection, no *Djnos*-positive cells were detected (Fig. 3B).

Having demonstrated that, in intact planarians, *DjRbAp48* RNAi induced a partial reduction in the number of neoblasts followed by the death of injected animals, we performed experiments aimed at investigating the neoblast proliferation rate in *DjRbAp48* RNAi animals. We counted the number of cells able to enter the M- and S-phases of the cell cycle. The number of mitotic cells was reduced with respect to the controls 20 days after RNAi treatment and then it remained relatively constant at the subsequent time points analyzed (Fig. 4B). The study of BrdU-positive cells confirmed the results obtained with the analysis of mitotic figures (Fig. 4C). The reduction in proliferating cells was also demonstrated by immunocytochemistry with the anti-H3P antibody in animals injected with *DjRbAp48* dsRNA (Fig. 4D,E). In addition, we performed FACS analysis of the irradiation-sensitive neoblast fractions (X1 and X2) (Hayashi et al., 2006; Reddien et al., 2005). Our findings revealed that the number of X1 and X2 cells in a neoblast-enriched cell fraction

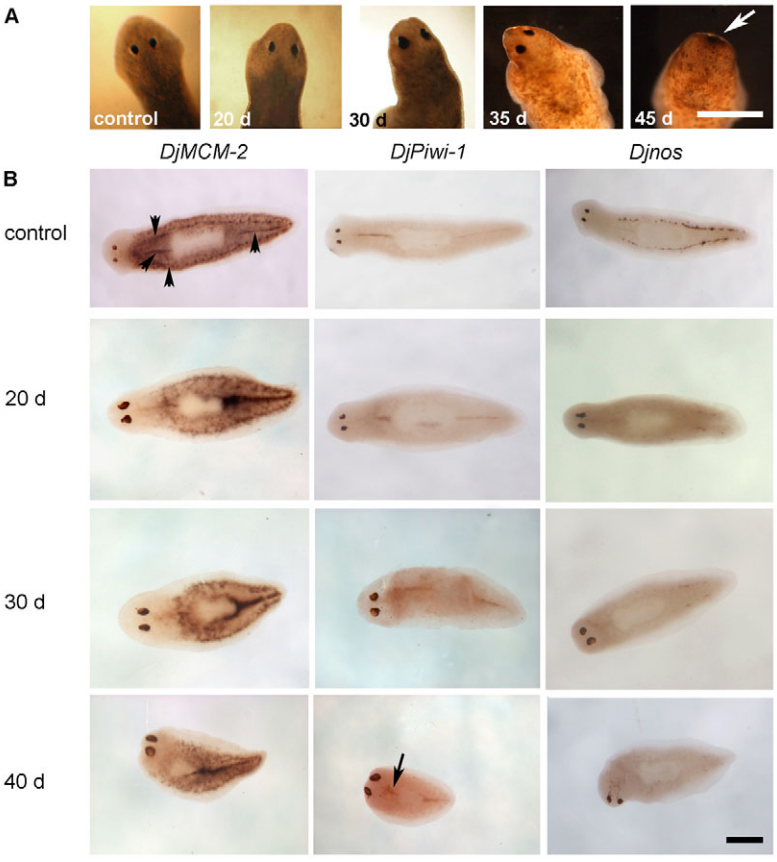

Fig. 3. *DjRbAp48* RNAi induces head regression and death in intact planarians. (**A**) Brightfield images of control and injected organisms at different days (d) after the first injection. The white arrow indicates the complete regression of the head in a *DjRbAp48*-injected planarian. (**B**) *DjMCM-2*, *DjPiwi-1* and *Djnos* expression visualized by whole-mount in situ hybridization in control and *DjRbAp48*-injected planarians at different days (d) after the first injection. Black arrowheads indicate neoblasts clustered along the body midline and dorsal lateral parenchyma in a control planarian. The arrow indicates *DjPiwi-1*-positive cells in front of the pharynx. Scale bar: 1 mm.

obtained from RNAi animals showing no head regression was reduced with respect to controls (Fig. 4F). FACS analysis also revealed that Xis cells, representing the X-ray-insensitive cell fraction, were only slightly reduced in number (10%). When we analyzed the number of total cells in a cell fraction enriched in differentiated cells (cell diameter >25 μm) obtained from controls and RNAi animals, we found a stronger reduction (30%) in differentiated (Xis) cells upon RNAi (Fig. 4F). To further verify the reduction in the number of differentiated cells after RNAi, we analysed the expression of some markers of differentiated cells by real-time RT-PCR [*DjIFb* (Tazaki et al., 2002); *DjMHC-B* (Kobayashi et al., 1998)] and whole-mount in situ hybridization (*DjAHNAK*). The results demonstrated that these markers are reduced in RNAi animals with respect to the controls (Fig. 5A,B). Histological analyses of *DjRbAp48*-injected animals, showing no gross morphological tissue regression, revealed a loss of tissue organization and a reduction in cell density (Fig. 5C-F). In addition, ultrastructural analysis showed the presence of apoptotic-like cells in animals 20 and 30 days after RNAi, but not in controls (Fig. 6A,B). These findings were confirmed by a DNA diffusion assay, which indicated that a significant number of apoptotic cells were present in neoblast-enriched cell fractions, but not in a suspension enriched in differentiated cells, obtained from animals killed 20 days after *DjRbAp48* RNAi with respect to the control planarians (Fig. 6C).

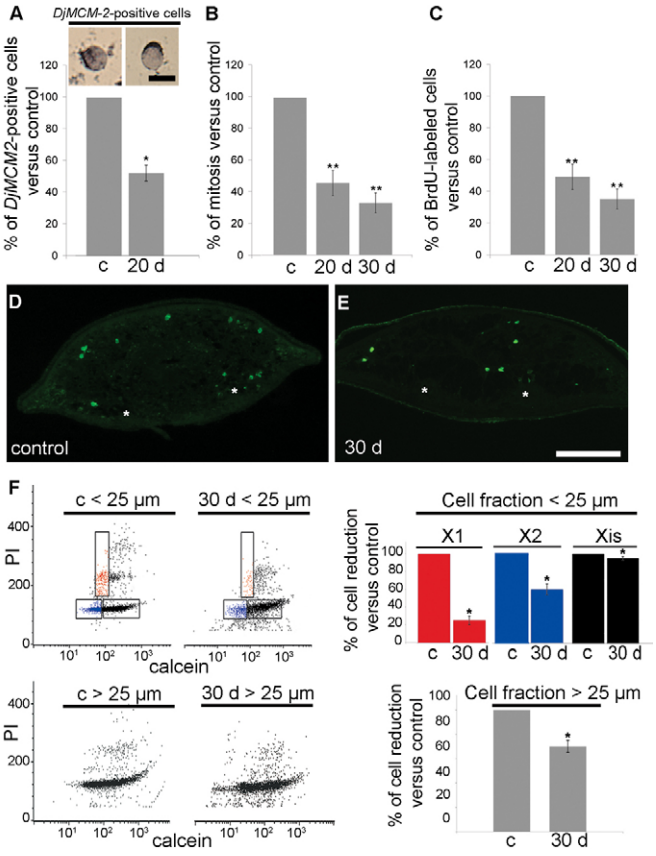

Fig. 4. Analysis of proliferating cells in intact *DjRbAp48* RNAi planarians. (**A**) Representative images of cells expressing the *DjMCM-2* marker. *DjMCM-2*-positive cells were counted in control (c) and RNAi animals (20 d). Values are expressed as percentages with respect to the control, to which the arbitrary value of 100% has been assigned. Each value is the mean ± standard deviation of three independent samples counted in duplicate. *Significant at $P<0.05$. (**B**,**C**) Analysis of mitotic and S-phase cells in control (c) and RNAi animals (20 d, 30 d). The number of cells able to enter the M- or S-phases of the cell cycle in a temporal window of 6 h was analyzed. Values are expressed as percentages with respect to the control planarians, to which the arbitrary value of 100% has been given. Each value is the mean ± standard deviation of at least three independent samples counted in duplicate. **Significant at $P<0.01$. (**D**,**E**) Distribution of mitotic cells by immunofluorescence using anti-H3P on transverse sections obtained from the body region anterior to the pharynx. The dorsal epithelium is towards the top. The asterisks indicate the nervous system. (**F**) FACS profile of PI- and calcein-labelled cells. The analysis was performed in a neoblast-enriched population of cells (diameter <25 μm) and in a population of cells enriched in differentiated cells (diameter >25 μm) obtained from control (c) and *DjRbAp48* RNAi (30 d) planarians 30 days after the first injection. X1 (red) and X2 (blue) populations are irradiation sensitive, Xis (black) is an X-ray-insensitive cell fraction. Statistical significance was assessed by Student's *t*-test. Scale bars: 10 μm (A); 200 μm (D,E).

DjRbAp48 RNAi effect on chromatin architecture

Because RbAp46 and RbAp48 factors are involved in chromatin metabolism at different levels, we wondered whether *DjRbAp48* silencing induced changes in neoblast chromatin. To this aim, we analysed the size and the amount of fluorescence emitted by Hoechst-stained neoblast nuclei obtained from animals killed 10 days after the first dsRNA injection, a time at which planarians do not show phenotypes (Fig. 7). The size of neoblast interphase nuclei was greater (10%) in RNAi animals compared to controls (data not shown) and the mean nuclear fluorescence of neoblasts in RNAi animals was 35% higher with respect to control interphase nuclei (Fig. 7A). Interestingly, a total nuclear fluorescence 65% higher than that of the controls was detected when the analysis was performed on a selected population of neoblasts with a nuclear area below 25,000 square pixels (Fig. 7D,E). Similarly, the treatment of planarians with NaBt, an agent known to be capable of altering chromatin structure (Davie, 2003), induced an increase in the total fluorescence of neoblast nuclei compared to the untreated controls (Fig. 7B,F,G). To test the effect of *DjRbAp48* RNAi on HDAC enzyme activity, we prepared nuclear extracts from RNAi animals and controls and performed an enzymatic activity assay. Fig. 7C shows that HDAC activity was not significantly affected by *DjRbAp48* silencing.

Discussion

A sequence of events produces a complete and functional regenerated planarian. After wound closure, stem cells proliferate, migrate and accumulate, thus generating a blastema. The neoblast progeny within the blastema differentiate and organize, and the lost body parts are then restored.

DjRbAp48 is expressed in neoblasts (Rossi et al., 2007) and animals silenced for its expression are not able to produce a blastema, as is the case for X-ray-treated animals devoid of neoblasts as a consequence of irradiation (Rossi et al., 2008). However, the loss of neoblasts is not the primary cause of regeneration failure in *DjRbAp48* RNAi animals. Indeed, we found that neoblasts still respond to the wound by proliferating and accumulating under the epithelium of *DjRbAp48*-silenced animals that are unable to generate a functional blastema.

Interestingly, regenerating *DjRbAp48* RNAi animals have a higher number of apoptotic cells with respect to control planarians. TEM analysis shows the presence of clusters of apoptotic-like cells with a high nucleus:cytoplasm ratio close to the wound, in a region corresponding to where the blastema is formed in control animals.

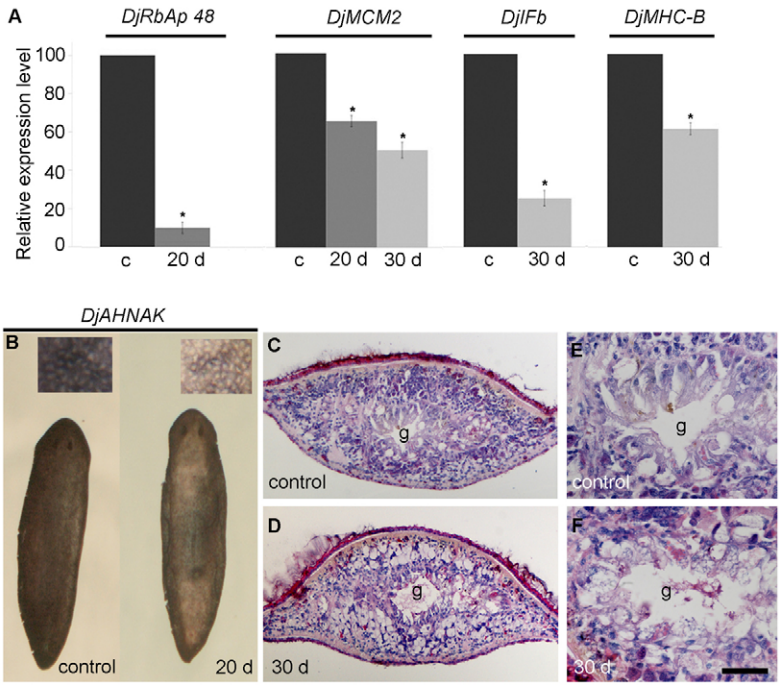

Fig. 5. Analysis of cellular differentiation in intact *DjRbAp48* RNAi planarians. (**A**) Real-time RT-PCR analysis. Expression levels are indicated in relative units, assuming the value of control planarians as 100. Each value is the mean ± standard deviation of three independent samples (n=3) analyzed in duplicate. *DjRbAp48* expression is strongly reduced after RNAi treatment. *DjMCM2* expression is reduced 20 days and 30 days (d) after RNAi. The expression level of the tissue-differentiated *DjIFb* and *DjMHC-B* markers is reduced after RNAi. *Significant at P<0.05. (**B**) *DjAHNAK* expression analyzed by whole-mount in situ hybridization. *DjAHNAK* was found to be expressed in the dorsal and ventral epidermis of RNAi animals (20 d) at lower levels with respect to the control planarians. (**C-F**) Histological analysis of transverse tissue sections stained with hematoxylin and eosin. The dorsal epithelium is towards the top. RNAi animals showed reduced cell density and tissue disorganization. g, gut. Statistical significance was assessed by Student's t-test. Scale bar: 1 mm (B); 100 µm (C,D); 50 µm (E,F).

TEM analysis also demonstrated the presence of apoptotic-like cells positive for BrdU distributed in clusters below the wound in RNAi animals: because neoblasts are the only proliferating cells in planarians, we hypothesize that these clusters of apoptotic cells are dying neoblasts.

Based on these observations, we conclude that *DjRbAp48* is not involved in neoblast maintenance and propose that it is required for neoblast progeny commitment and/or differentiation. A possible role for *DjRbAp48* in the control of neoblast progeny is also supported by evidence that this gene is expressed in the blastema region of regenerating wild-type animals. In *DjRbAp48* RNAi animals, neoblasts are activated by wounding, but they cannot undergo differentiation and so they die by apoptosis. The remaining neoblasts proliferate to the last, trying to produce a blastema but, as they fail, RNAi animals die. Consistent with the idea that *DjRbAp48* is not involved in neoblast maintenance, regenerating animals silenced for a gene that is known to be involved in neoblast maintenance, such as *DjPum*, do not show accumulated neoblasts below the wound epidermis (Salvetti et al., 2005). Accordingly, neoblasts are lost during regeneration after silencing of *Smed-bruli*, another gene required for stem-cell maintenance (Guo et al., 2006).

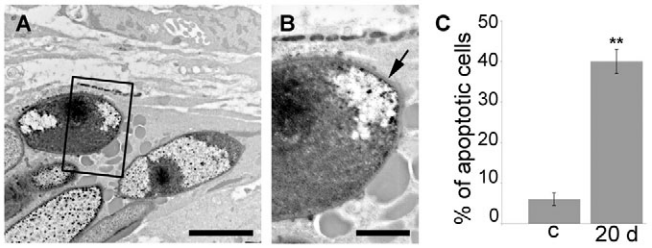

Fig. 6. Analysis of apoptosis in intact *DjRbAp48* RNAi planarians. (**A**) Micrograph of a cluster of apoptotic-like cells in *RbAp48* RNAi animals. (**B**) Magnification of A (black box) showing chromatin condensation. The arrow indicates the plasma membrane. (**C**) DNA diffusion assay of control (c) and *DjRbAp48* RNAi (20 d) planarians 20 days after the first injection. Dissociated cells were prepared from a pool of three planarians per sample. Cells classified as type IV were considered apoptotic. Apoptotic cells were found in the cell fraction obtained from *DjRbAp48* RNAi animals by filtration through a 20 µm pore-size mesh, a cell fraction that mainly contains neoblasts and differentiating neoblasts. Values are expressed as the percentage of apoptotic cells with respect to the total counted cells. Each value is the average ± standard deviation of at least three independent samples counted in duplicate. We counted 50 cells for each sample. **Significant at P<0.01. Statistical significance was assessed by Student's t-test. Scale bars: 3 µm (A); 1 µm (B).

Our hypothesis is also supported by findings obtained in intact RNAi animals. Although *DjRbAp48*-silenced animals show a phenotype typical of irradiated animals, a significant number of neoblasts could always be detected in intact RNAi animals, as well as in animals showing head regression, as indicated by the expression of the neoblast molecular markers *DjMCM2*, *DjPiwi-1* and *Djnos*, as well as by counting M- and S-phase neoblasts. In addition, FACS analysis demonstrated that, although the X1 fraction, mainly containing proliferating cells, and the X2 fraction, containing a limited number of non-proliferating cells, are reduced after RNAi, a significant number of neoblasts are always detected in intact *DjRbAp48*-silenced animals. In particular, we found that most scattered *DjMCM2*-expressing neoblasts in the parenchyma, the highly proliferating transit neoblast progeny (Salvetti et al., 2009), disappeared 20 days after RNAi, whereas clustered neoblasts along the body midline were always detected, as also found in animals exhibiting phenotypes. Although we failed to detect an antero-posterior gradient in *DjRbAp48* expression, neoblasts located in the anterior body regions seem to disappear more rapidly than those located in the posterior regions after RNAi. A possible explanation is that complex organs and systems, which are mainly located in the anterior region, might be subjected to greater cell turnover than those located in the posterior body region, as has been hypothesized by Oviedo and Levin (Oviedo and Levin, 2007).

Why do intact RNAi animals die? Bearing in mind the results obtained in regenerating RNAi animals, we propose that intact RNAi

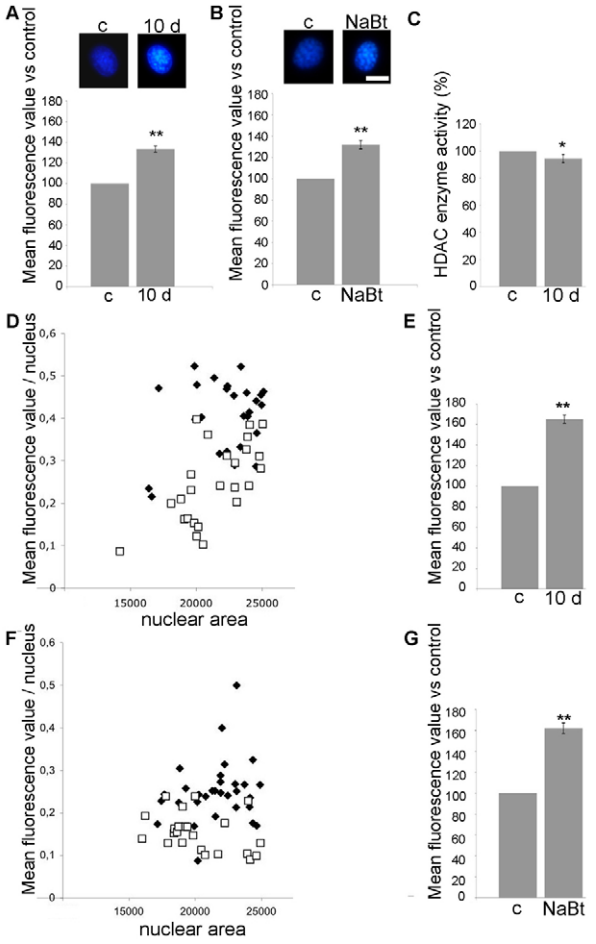

Fig. 7. Analysis of interphase neoblast nuclei in intact *DjRbAp48* RNAi planarians. Representative images of interphase neoblast nuclei obtained (**A**) from control (c) and *DjRbAp48* RNAi (10 d) animals 10 days after the first injection, and (**B**) from control (c) and NaBt-treated (NaBt) animals. Nuclei are stained with the dye Hoechst No. 33342. The mean nuclear fluorescence values are expressed as the percentage with respect to the control (c), to which the arbitrary value of 100% has been assigned. Each value is the average ± standard deviation of at least 60 independent nuclei. **Significant at $P<0.01$. (**C**) HDAC enzyme activity measured in nuclear extracts obtained from control (c) and *DjRbAp48* RNAi (10 d) animals 10 days after the first injection. The enzyme activity is expressed as the percentage with respect to the control (c), to which the arbitrary value of 100% has been assigned. *Significant at $P<0.05$. (**D**,**E**) Analysis of the mean nuclear fluorescence in a subpopulation of neoblasts obtained from controls and RNAi- treated animals. (**F**,**G**) Analysis of the mean nuclear fluorescence in a subpopulation of neoblasts obtained from controls and NaBt-treated animals. A white square corresponds to one control nucleus; a black rhombus corresponds to one RNAi nucleus or to one NaBt-treated nucleus. Area is indicated in square pixels and calculated by Image J software. The mean nuclear fluorescence values are expressed as the percentage with respect to the control (c), to which the arbitrary value of 100% has been assigned. Each value is the average ± standard deviation of at least 25 independent nuclei. **Significant at $P<0.01$. Statistical significance was assessed by Student's *t*-test. Scale bars: 10 µm.

animals die as they cannot replace lost differentiated cells because neoblast progeny cannot undergo cell differentiation. Although no information is available about the life-time of differentiated cells in planarians, our hypothesis is supported by the evidence that intact RNAi animals, containing proliferating neoblasts in their parenchyma and showing no evident tissue regression, have tissue disorganization. Moreover, they show induction of apoptosis and reduction in both cell density and number of differentiated cells, as well as in the expression of differentiated tissue markers. Even if mitosis had been found at all the analysed time points, the neoblast progeny might fail to undergo cell differentiation and maintain physiological cell turnover, which finally causes the death of injected animals. A phenotype resembling that of irradiated animals lacking neoblasts has also been obtained by silencing *smedwi-2*, even though neoblasts are present in RNAi animals (Reddien et al., 2005). These authors suggested that, in RNAi animals, the neoblast progeny migrates to the sites of cell turnover, but fails at replacing aged tissue.

Our results indicate that *DjRbAp48* silencing induces a change in nuclear size and fluorescence, suggesting that *DjRbAp48* might be an epigenetic factor. A possibility is that *DjRbAp48*, like other retinoblastoma-associated proteins, might control the expression of genes necessary for neoblast differentiation by influencing chromatin architecture. Indeed, the coordinated activation and silencing of genes during cellular differentiation requires the large-scale remodelling of chromatin architecture to long-term silence specific genes (Cremer and Cremer, 2001). The RbAp46 and RbAp48 factors are components of several chromatin-remodelling complexes and it has been reported that, in other organisms, RbAp48 and E2F-1 are physically associated in the presence of Rb and HDAC, suggesting that RbAp48 could be involved in transcriptional repression of E2F-responsive genes (Nicolas et al., 2000). However, the functions of RbAp46 and RbAp48 in chromatin-remodelling complexes are not yet clearly established. Our data suggest that *DjRbAp48* silencing does not significantly affect HDAC activity. A possibility is that DjRbAp48 is not functionally linked to HDAC and/or that it might be a component of chromatin-remodelling complexes that do not contain HDAC. Although additional studies are necessary to understand at which level DjRbAp48 might affect chromatin metabolism, our findings represent the first evidence that a retinoblastoma-associated protein factor is involved in adult stem-cell biology in vivo.

Materials and Methods

Animals

Planarians used in this work belong to the species *D. japonica*, asexual strain GI (Orii et al., 1993). Animals were kept in autoclaved stream water at 18°C and starved for at least 2 weeks before being used in the experiments. Regenerating fragments were obtained by transection between auricles and pharynx, or tail and pharynx.

Isolation of *DjRbAp48*

The expressed sequence tag (EST) clone Gi32900731, obtained from a *D. japonica* head EST collection (Mineta et al., 2003), is a homologue of factor RbAp48 (Rossi et al., 2007). The full-length clone, named *DjRbAp48* (accession number: FM210472), was obtained by 5′ and 3′ RACE (rapid amplification of cDNA ends) using the SMART RACE cDNA amplification kit (Clontech) according to the manufacturer's instructions. Homology searches were performed using BLAST (Altschul et al., 1990).

RNAi experiments

Double-stranded RNA (dsRNA) of *DjRbAp48* was obtained as previously described (Salvetti et al., 2005) by amplification of the clone Gi32900731 using the following T7 promoter adapted primers: forward 5′-TAATACGACTCACTATAGGGAGA-TGATTTGGTAATGACTCATGCT-3′; reverse 5′-TAATACGACTCACTATAGG-GAGACCTTTTAATCTAAGATCGG-3′.

Intact planarians were injected with *DjRbAp48* dsRNA (RNAi animals) for four consecutive days and then once a week until the day of the experiment using the Nanoject Microinjector (Drummond). For first regeneration experiments, animals were injected for four consecutive days, amputated on the fifth day and allowed to regenerate. For second regeneration experiments, the newly formed blastema was eliminated on the seventh day after the first injection. For third and fourth regeneration experiments, tail fragments were amputated on the eleventh and fifteenth days after the first injection, respectively. The reduction of *DjRbAp48* endogenous transcripts in injected specimens was assessed by real-time PCR. Planarians injected with

β-galactosidase dsRNA or water were used as negative controls. Injected animals were observed daily with a Wild Heerbrugg stereomicroscope.

BrdU labelling and detection

Control planarians and *DjRbAp48* RNAi animals, 20 or 30 days after the first dsRNA injection, were injected with 10 mM BrdU. The number of BrdU-labelled neoblasts was estimated 6 hours after BrdU injection as previously described (Salvetti et al., 2009). Briefly, about 1×10^4 nuclei were examined for each preparation, and only nuclei with fine-grained bright florescence through the nuclear matrix and bright perinuclear chromatin staining were considered positive. A total of 10 µl of cell suspension was examined using a hemocytometer to count total cell number. The relative number of BrdU-positive nuclei was calculated by dividing the absolute number of positive nuclei by the number of total cells. Three independent samples were analyzed in duplicate for each experimental condition. Slides were scored with a Zeiss Axioplan photomicroscope.

To detect S-phase cells by TEM, *DjRbAp48* RNAi animals were cut, injected with BrdU 30 minutes later and allowed to regenerate. Animals were then fixed 3 and 6 days after BrdU injection and processed for TEM.

Analysis of mitosis

Intact control and *DjRbAp48* RNAi planarians, 20 or 30 days after the first dsRNA injection, as well as control and *DjRbAp48* RNAi head and tail fragments 4 days after the second amputation, were treated with 0.3% colchicine in stream water for six hours, dissociated in 250 µl of a glycerol:acetic acid:distilled water solution (1:1:13) for 20 hours at 4°C, and then stained with 20 µg/ml Hoechst No. 33342. A total of 20 µl of cell suspension was placed on a microscope slide, dried for a couple of hours and then mounted for microscope analysis. Slides were scored with a Zeiss Axioplan photomicroscope to count the number of mitotic figures. About 1×10^4 nuclei were examined for each preparation. A total of 10 µl of cell suspension was used in a hemocytometer to calculate the mitotic index, that is, the number of cells undergoing mitosis divided by the total cell number. Three independent samples were analyzed in duplicate for each experimental condition. For experiments on regenerating animals, the mitotic index was calculated 4 days after the first or the second transection, as described above.

In situ hybridization

Whole-mount in situ hybridization was performed as described in Rossi et al. (Rossi et al., 2007). DNA templates for *DjPiwi-1* were prepared as previously described in Rossi et al. (Rossi et al., 2006), and *DjAHNAK* and *DjRbAp48* templates were obtained according to Rossi et al. (Rossi et al., 2007). *DjMCM2* and *DjSyt* templates were prepared according to Salvetti et al. (Salvetti et al., 2000), and the *Djnos* template was obtained as described in Salvetti et al. (Salvetti et al., 2009). The *Djinx1* DNA fragment, corresponding to nucleotide positions 285-669 of the *Djinx1* sequence (Nogi and Levin, 2005), was obtained by RT-PCR using the following primers: *Djinx1* forward 5′-CAATCCCGAAACTGCAAGAAA-3′; *Djinx1* reverse 5′-TAATACGACTCACTATAGGGAGACATATTTTCTACTACCGAATCC-3′. Purified amplification products or digested plasmids were in vitro transcribed to obtain digoxigenin (DIG)-labelled RNA probes using the DIG-RNA labelling kit (Roche).

Immunohistochemistry

Immunohistochemistry on tissue sections was performed using anti-phosphohistone H3 antibodies (anti-H3P; Upstate Biotech) as described previously (Sato et al., 2006). Anti-H3P staining was revealed using a fluorescein-isothiocyanate-conjugated anti-rabbit antibody (Molecular Probes) (1:200 dilution in PBS containing 1% BSA). Control sections were incubated in 10% goat serum with no primary antibody. All slides were observed under a Zeiss Axioplan fluorescence microscope.

Transmission electron microscopy

TEM was performed as previously described in Salvetti et al. (Salvetti et al., 2005). Briefly, planarians were fixed with a 2.5% glutaraldehyde solution in 0.1 M cacodylate buffer and post-fixed with 2% osmium tetroxide. Ultrathin sections were stained with uranyl acetate and lead citrate, and observed with a Jeol 100 SX transmission electron microscope.

Immunogold labelling of S-phase neoblasts was performed as described in Bode et al. (Bode et al., 2006). Planarians were fixed 3 and 6 days after amputation, and embedded as described in Salvetti et al. (Salvetti et al., 2002). Sections were incubated with 1/100 anti-BrdU monoclonal antibody (BD Pharmingen) in 0.1% gelatin, 0.5% BSA and 0.05% Tween-20 (blocking buffer) for 12 hours. After washing, sections were incubated for 1 hour with the 10 nm gold-conjugated secondary antibody (BBInternational) (1:30 in blocking buffer). Sections were then stained with uranyl acetate and lead citrate. Negative controls were incubated with the secondary antibody only.

DNA diffusion assay

Intact control and *DjRbAp48* RNAi animals 20 days after injection, or regenerating control and RNAi planarians 4 days after the second transection (that is, 11 days after the first dsRNA injection) were dissociated into individual cells as described in Salvetti et al. (Salvetti et al., 2005). Neoblast-enriched fractions were obtained by serial filtration through nylon meshes of decreasing pore size (150, 50 and 25 µm; Millipore). Cell differentiated enriched fractions were obtained using pore sizes greater than 25 µm. A DNA diffusion assay was performed to quantify apoptosis, as described by Singh (Singh, 2005). Briefly, cells were mixed with agarose and lysed with 2.5 M NaCl, 10 mM TrisHCl, 0.1 M EDTA, 1% Triton-X-100, 10% DMSO, pH 10. The diffused DNA fragments were detected by staining with the fluorescent dye ethidium bromide. Apoptotic cells show a circular gradient of granular DNA with a dense central zone and a lighter and hazy outer zone, giving the overall appearance of a halo.

FACS analysis

Intact control and *DjRbAp48* RNAi animals showing no evident tissue regression were dissociated and analysed by FACS as previously described (Salvetti et al., 2009). Briefly, a cell suspension enriched in neoblasts by filtration through a 25 µm nylon mesh (cell diameter less than 25 µm) and a cell suspension enriched in differentiated cells with a diameter greater than 25 µm were incubated with calcein AM (0.5 µg/ml; Sigma), fixed in 70% ethanol, and then incubated for 30 minutes at room temperature in PBS containing propidium iodide (PI, 50 µg/ml; Roche), RNAse (6.25 µg/ml; Roche) and IGEPAL CA-630 (0.5% v/v; Sigma-Aldrich). FACS analysis of calcein staining versus PI incorporation was performed by a FACScalibur cytofluorimeter (Becton Dickinson) and data were analyzed by CELL Quest analysis software (Becton Dickinson). Cellular debris was excluded by forward-angle light scatter (FSC) and side-angle light scatter (SSC) analysis.

Real-time RT-PCR

Real-time RT-PCR was performed using the Brilliant II SYBRGreeen QPCR master mix (Stratagene) to amplify 20 ng of cDNA reverse transcribed from total RNA. The constitutively expressed elongation factor gene *DjEF2* was used for normalization.

Primers used in the amplification reaction are as follows: *DjMCM2* forward 5′-TCTGGCGATCTAAGAAGAGG-3′; *DjMCM2* reverse 5′-ATCCCAATGTTTCAC-CTGCC3′; *DjRbAp48* forward 5′-TGATTTGGTAATGACTCATGCT-3′; *DjRbAp48* reverse 5′-ATCTGTGGGTATATGAGCAGT-3′; *DjIfb* forward 5′-GGGGTAAA-GAAACTGCCAGA-3′; *DjIfb* reverse 5′-CTGAGTAGCATCATTTAATTCC-3′; *DjMHC-b* forward 5′-CAACATCATCAACGTGAATTGG-3′; *DjMHC-b* reverse 5′-AGCTCATTAAGTTTATCAACGG-3′; *DjEF2* forward 5′-GCGTAAATGGT-TACCAGCAG-3′; *DjEF2* reverse 5′-GACACGGCAATTTCATCATCT-3′.

Cytological analysis

A suspension of neoblast-enriched cells was obtained as described in Salvetti et al. (Salvetti et al., 2005) from a pool (n=6) of intact control and RNAi animals killed 10 days after the first injection. Cells were spread on microscope slides, air dried and stained with 20 µg/ml Hoechst No. 33342. The fluorescence patterns were examined with a Zeiss Axioplan microscope and images were recorded with a Nikon camera. Digital images were quantified using the program Image J (Abramoff et al., 2004). Total nuclear size and fluorescence were determined for at least 60 representative nuclei obtained from two independent samples. As control, a suspension of cells enriched in neoblasts was obtained from a pool of animals treated with 30 mM NaBt (sodium butyrate), an agent that alters chromatin structure, for 24 hours. The maximal NaBt dose that does not produce evident morphological defects was established by dose-effect experiments at different NaBt concentrations (from 5 mM to 35 mM). As negative control, we used a suspension of cells enriched in neoblasts obtained from a pool of animals treated with vehicle.

Isolation of nuclear extracts and HDAC activity assay

A total of 60 *DjRbAp48* RNAi animals and 60 controls were homogenized in 1 ml cold lysis buffer (10 mM Tris-HCl, pH 7.4, 10 mM NaCl, 15 mM $MgCl_2$, 0.1 mM EGTA, 250 mM sucrose). After the addition of NP-40 (0.5% final concentration), the homogenates were vortexed for 10 seconds and kept on ice for 15 minutes. The nuclei were collected by centrifugation through 4 ml of cold sucrose cushion (30% sucrose, 10 mM Tris-HCl, pH 7.5, 10 mM NaCl, 3 mM $MgCl_2$) at 1300 ***g*** for 10 minutes at 4°C, resuspended in 400 µl 10 mM Tris-HCl, pH 7.4, 10 mM NaCl, and centrifuged at 1300 ***g*** for 10 minutes at 4°C. Nuclear pellets were resuspended in 50 ml 1.5× RIPA buffer (80 mM Tris-HCl, pH 7.5, 800 mM NaCl, 0.4% deoxycholic acid, 1.6% NP-40, 1.6 mM EDTA), incubated on ice for 30 minutes, and centrifuged at 10,000 ***g*** for 10 minutes at 4°C (modified from Di Renzo et al., 2007). The supernatant, containing nuclear proteins, was stored in aliquots at –80°C until use. Protein concentration was determined by Bradford assay (Bio-Rad). To determine the HDAC activity of the extracts, 15 µl of each sample, containing about 30 µg protein, was assayed using the HDAC Assay Kit (Fluorometric Detection) from Upstate, according to manufacturer's instructions.

We thank Cristina Tocchini and Claudio Ghezzani for histological and TEM assistance, respectively. We are grateful to Awatef Allouch for the HDAC assay and Marco Nigro for assistance with the DNA diffusion assay. Grant sponsor: University of Pisa.

Supplementary material available online at
http://jcs.biologists.org/cgi/content/full/123/5/690/DC1

References

Abramoff, M. D., Magelhaes, P. J. and Ram, S. J. (2004). Image processing with ImageJ. *Biophotonics International* **11**, 36-42.

Altschul, S. F., Gish, W., Miller, W., Myers, E. W. and Lipman, D. J. (1990). Basic local alignment search tool. *J. Mol. Biol.* **215**, 403-410.

Azuara, V., Perry, P., Sauer, S., Spivakov, M., Jørgensen, H. F., John, R. M., Gouti, M., Casanova, M., Warnes, G., Merkenschlager, M. et al. (2006). Chromatin signatures of pluripotent cell lines. *Nat. Cell Biol.* **8**, 532-538.

Baguna, J., Salo, E. and Auladell, C. (1989). Regeneration and pattern formation in planarians: III. Evidence that neoblasts are totipotent stem cells and the source of blastema cells. *Development* **107**, 77-86.

Bar-Sagi, D. and Hall, A. (2000). Ras and Rho GTPases: a family reunion. *Cell* **103**, 227-238.

Bode, A., Salvenmoser, W., Nimeth, K., Mahlknecht, M., Adamski, Z., Rieger, R. M., Peter, R. and Ladurner, P. (2006). Immunogold-labeled S-phase neoblasts, total neoblast number, their distribution, and evidence for arrested neoblasts in *Macrostomum lignano* (Platyhelminthes, Rhabditophora). *Cell Tissue Res.* **325**, 577-587.

Boyer, L. A., Mathur, D. and Jaenisch, R. (2006a). Molecular control of pluripotency. *Curr. Opin. Genet. Dev.* **16**, 455-462.

Boyer, L. A., Plath, K., Zeitlinger, J., Brambrink, T., Medeiros, L. A., Lee, T. I., Levine, S. S., Wernig, M., Tajonar, A., Ray, M. K. et al. (2006b). Polycomb complexes repress developmental regulators in murine embryonic stem cells. *Nature* **441**, 349-353.

Chamberlain, S. J., Yee, D. and Magnuson, T. (2008). Polycomb repressive complex 2 is dispensable for maintenance of embryonic stem cell pluripotency. *Stem Cells* **26**, 1496-1505.

Cox, A. D. and Der, C. J. (2003). The dark side of Ras: regulation of apoptosis. *Oncogene* **22**, 8999-9006.

Cremer, T. and Cremer, C. (2001). Chromosome territories, nuclear architecture and gene regulation in mammalian cells. *Nat. Rev. Genet.* **2**, 292-301.

Davie, J. R. (2003). Inhibition of histone deacetylase activity by butyrate. *J. Nutr.* **133**, 2485-2493.

Di Renzo, F., Cappelletti, G., Broccia, M. L., Giovini, E. and Menegola, E. (2007). Boric acid inhibits histone deacetylases: a suggested mechanism to explain boric acid-related teratogenicity. *Toxicol. Appl. Pharmacol.* **220**, 178-185.

Downward, J. (2003). Targeting RAS signalling pathways in cancer therapy. *Nat. Rev. Cancer* **3**, 11-22.

Guo, T., Peter, A. H. and Newmark, P. A. (2006). A bruno-like gene is required for stem cell maintenance. *Dev. Cell* **11**, 159-169.

Hancock, J. F. (2003). Ras proteins: different signals from different locations. *Nat. Rev. Mol. Cell. Biol.* **4**, 373-384.

Hayashi, T., Asami, M., Higuchi, S., Shibata, N. and Agata, K. (2006). Isolation of planarian X-ray-sensitive stem cells by fluorescence-activated cell sorting. *Dev. Growth Differ.* **48**, 371-380.

Hennig, L., Taranto, P., Walser, M., Schönrock, N. and Gruissem, W. (2003). Arabidopsis MSI1 is required for epigenetic maintenance of reproductive development. *Development* **130**, 2555-2565.

Kamminga, L. M., Bystrykh, L. V., de Boer, A., Houwer, S., Douma, J., Weersing, E., Dontje, B. and de Haan, G. (2006). The Polycomb group gene Ezh2 prevents hematopoietic stem cell exhaustion. *Blood* **107**, 2170-2179.

Kobayashi, C., Kobayashi, S., Orii, H., Watanabe, K. and Agata, K. (1998). Identification of two distinct muscles in the planarian *Dugesia japonica* by their expression of myosin chain genes. *Zool. Sci.* **15**, 861-869.

Lee, T. I., Jenner, R. G., Boyer, L. A., Guenther, M. G., Levine, S. S., Kumar, R. M., Chevalier, B., Johnstone, S. E., Cole, M. F., Isono, K. et al. (2006). Control of developmental regulators by Polycomb in human embryonic stem cells. *Cell* **125**, 301-313.

Loyola, A. and Almouzni, G. (2004). Histone chaperones, a supporting role in the limelight. *Biochim. Biophys. Acta.* **1677**, 3-11.

Lu, X. and Horvitz, H. R. (1998). lin-35 and lin-53, two genes that antagonize a *C. elegans* Ras pathway, encode proteins similar to Rb and its binding protein RbAp48. *Cell* **95**, 981-991.

Mineta, K., Nakazawa, M., Cebria, F., Ikeo, K., Agata, K. and Gojobori, T. (2003). Origin and evolutionary process of the CNS elucidated by comparative genomics analysis of planarian ESTs. *Proc. Natl. Acad. Sci. USA* **100**, 7666-7671.

Morgan, T. H. (1898). Experimental studies of the regeneration of *Planaria maculata*. *Arch. Entwm. Org.* **7**, 364-397.

Neer, E. J., Schmidt, C. J., Nambudripad, R. and Smith, T. F. (1994). The ancient regulatory-protein family of WD-repeat proteins. *Nature* **371**, 297-300.

Newmark, P. A. and Sánchez Alvarado, A. (2000). Bromodeoxyuridine specifically labels the regenerative stem cells of planarians. *Dev. Biol.* **220**, 142-153.

Nicolas, E., Morales, V., Magnaghi-Jaulin, L., Harel-Bellan, A., Richard-Foy, H. and Trouche, D. (2000). RbAp48 belongs to the histone deacetylase complex that associates with the retinoblastoma protein. *J. Biol. Chem.* **275**, 9797-9804.

Nogi, T. and Levin, M. (2005). Characterization of innexin gene expression and functional roles of gap-junctional communication in planarian regeneration. *Dev. Biol.* **15**, 314-335.

Orii, H., Agata, K. and Watanabe, K. (1993). POU-domain genes in planarian *Dugesia japonica*: the structure and expression. *Biochem. Biophys. Res. Commun.* **192**, 1395-1402.

Orii, H., Sakurai, T. and Watanabe, K. (2005). Distribution of the stem cells (neoblasts) in the planarian *Dugesia japonica*. *Dev. Genes Evol.* **215**, 143-157.

Oviedo, N. J. and Levin, M. (2007). smedinx-11 is a planarian stem cell gap junction gene required for regeneration and homeostasis. *Development* **134**, 3121-3131.

Parthun, M. R., Widom, J. and Gottschling, D. E. (1996). The major cytoplasmic histone acetyltransferase in yeast: links to chromatin replication and histone metabolism. *Cell* **87**, 85-94.

Philpott, A., Krude, T. and Laskey, R. (2000). Nuclear chaperones. *Semin. Cell Dev. Biol.* **11**, 7-14.

Qian, Y. W. and Lee, E. Y. H. P. (1995). Dual retinoblastoma-binding proteins with properties related to a negative regulator of Ras in yeast. *J. Biol. Chem.* **270**, 25507-25513.

Qian, Y. W., Wang, Y. C., Hollingsworth, R. E., Jr, Jones, D., Ling, N. and Lee, E. Y. (1993). A retinoblastoma-binding protein related to a negative regulator of Ras in yeast. *Nature* **364**, 648-652.

Reddien, P. W., Oviedo, N. J., Jennings, J. R., Jenkin, J. C. and Sánchez Alvarado, A. (2005). SMEDWI-2 is a PIWI-like protein that regulates planarian stem cells. *Science* **310**, 1327-1330.

Rossi, L., Salvetti, A., Lena, A., Batistoni, R., Deri, P., Pugliesi, C., Loreti, E. and Gremigni, V. (2006). DjPiwi-1, a member of the PAZ-Piwi gene family, defines a subpopulation of planarian stem cells. *Dev. Genes Evol.* **216**, 335-346.

Rossi, L., Salvetti, A., Marincola, F. M., Lena, A., Deri, P., Mannini, L., Batistoni, R., Wang, E. and Gremigni, V. (2007). Deciphering the molecular machinery of stem cells: a look at the neoblast gene expression profile. *Genome Biol.* **8**, R62.

Rossi, L., Salvetti, A., Batistoni, R., Deri, P. and Gremigni, V. (2008). Planarians, a tale of stem cells. *Cell Mol. Life Sci.* **65**, 16-23.

Ruggieri, R., Tanaka, K., Nakafuku, M., Kaziro, Y., Toh-e, A. and Matsumoto, K. (1989). MSI1, a negative regulator of the RAS-cAMP pathway in *Saccharomyces cerevisiae*. *Proc. Natl. Acad. Sci. USA* **86**, 8778-8782.

Salvetti, A., Rossi, L., Deri, P. and Batistoni, R. (2000). An MCM2-related gene is expressed in proliferating cells of intact and regenerating planarians. *Dev. Dyn.* **218**, 603-614.

Salvetti, A., Lena, A., Rossi, L., Deri, P., Cecchettini, A., Batistoni, R. and Gremigni, V. (2002). Characterization of DeY1, a novel Y-box gene specifically expressed in differentiating male germ cells of planarians. *Gene Expr. Patterns* **2**, 195-200.

Salvetti, A., Rossi, L., Lena, A., Batistoni, R., Deri, P., Rainaldi, G., Locci, M. T., Evangelista, M. and Gremigni, V. (2005). DjPum, a homologue of *Drosophila* Pumilio, is essential to planarian stem cell maintenance. *Development* **132**, 1863-1874.

Salvetti, A., Rossi, L., Bonuccelli, L., Lena, A., Pugliesi, C., Rainaldi, G., Evangelista, M. and Gremigni, V. (2009). Adult stem cell plasticity: neoblast repopulation in non-lethally irradiated planarians. *Dev. Biol.* **328**, 305-314.

Sato, K., Shibata, N., Orii, H., Amikura, R., Sakurai, T., Agata, K., Kobayashi, S. and Watanabe, K. (2006). Identification and origin of the germline stem cells as revealed by the expression of nanos-related gene in planarians. *Dev. Growth Differ.* **48**, 615-628.

Scuto, A., Zhang, H., Zhao, H., Rivera, M., Yeatman, T. J., Jove, R. and Torres-Roca, J. F. (2007). RbAp48 regulates cytoskeletal organization and morphology by increasing K-Ras activity and signaling through mitogen-activated protein kinase. *Cancer Res.* **67**, 10317-10324.

Shields, J. M., Pruitt, K., McFall, A., Shaub, A. and Der, C. J. (2000). Understanding Ras: "it ain't over 'til it's over." *Trends Cell Biol.* **10**, 147-154.

Singh, N. P. (2000). A simple method for accurate estimation of apoptotic cells. *Exp. Cell Res.* **256**, 328-337.

Singh, N. P. (2005). Apoptosis assessment by the DNA diffusion assay. *Methods Mol. Med.* **111**, 55-67.

Taunton, J., Hassig, C. A. and Schreiber, S. L. (1996). A mammalian histone deacetylase related to the yeast transcriptional regulator Rpd3p. *Science* **272**, 408-411.

Tazaki, A., Gaudieri, S., Ikeo, K., Gojobori, T., Watanabe, K. and Agata, K. (1999). Neural network in planarian revealed by an antibody against planarian synaptogamin homologue. *Biochem. Biophys. Res. Commun.* **260**, 426-432.

Tazaki, A., Kato, K., Orii, H., Agata, K. and Watanabe, K. (2002). The body margin of the planarian *Dugesia japonica*: characterization by the expression of an intermediate filament gene. *Dev. Genes Evol.* **212**, 365-373.

Verreault, A., Kaufman, P. D., Kobayashi, R. and Stillman, B. (1996). Nucleosome assembly by a complex of CAF-1 and acetylated histones H3/H4. *Cell* **87**, 95-104.

Wei, Y., Mizzen, C. A., Cook, R. G., Gorovsky, M. A. and Allis, C. D. (1998). Phosphorylation of histone H3 at serine 10 is correlated with chromosome condensation during mitosis and meiosis in *Tetrahymena*. *Proc. Natl. Acad. Sci. USA* **95**, 7480-7484.

Wolff, E. and Dubois, F. (1948). Sur la migration des cellules de régénération chez les planaires. *Rev. Suisse Zool.* **55**, 218-227.